

with magnitudes of 5% to the 3D grid nodes. Synthetic data were calculated for the checkerboard model. Then we added random errors to the synthetic data and inverted them with the same algorithm that we used for the observed data. The inverted image of the checkerboard suggests where the resolution is good and where it is poor. The checkerboard resolution tests and other synthetic tests we conducted showed that both the high-velocity Tonga slab and the low-velocity back arc and mantle wedge were reliably resolved and that there was no trade-off between them.

12. Y. Tatsumi, *J. Geophys. Res.* **94**, 4697 (1989); J. H. Davies and D. J. Stevenson, *ibid.* **97**, 2037 (1992).
13. Y. Zhang and T. Tanimoto, *Nature* **355**, 45 (1992); T. Tanimoto and D. J. Stevenson, *J. Geophys. Res.* **99**, 4549 (1994).
14. Y. Shen and D. W. Forsyth, *J. Geophys. Res.* **100**, 2211 (1995).
15. Y. Xu and D. Wiens, *ibid.*, in press. To invert regional wave forms we used a nonlinear inversion method that adopts a reflectivity formalism (28) to compute the partial derivatives. This method allows the entire regional distance (400- to 1500-km range) wave form to be inverted from *P* wave arrival to surface waves at frequencies between 0.01 and 0.055 Hz. Broadband seismograms from earthquakes of 10 to 240 km deep that propagate almost entirely within one of the tectonic regions of the southwest Pacific were used in the wave form inversion. Parameter variances and resolution tests suggest that the results are well constrained to depths of about 200 km. The *S* wave velocities from the wave form inversion and the *P* wave velocities from the tomography would not necessarily show the same structure. The larger total heterogeneity from the wave form inversion may result from a greater effect of partial melt beneath the Lau back arc on *S* wave velocity than on *P* wave velocity (9, 29).
16. W. Su, R. L. Woodward, A. M. Dziewonski, *Nature* **360**, 149 (1992).
17. G. Nolet and A. Zielhuis, *J. Geophys. Res.* **99**, 15813 (1994); G. Nolet, in *Processes of Deep Earth and Planetary Volatiles*, K. Farley, Ed. (American Institute of Physics, New York, 1995), pp. 22–32.
18. A. B. Thompson, *Nature* **358**, 295 (1992); H. Staudigel and S. D. King, *Earth Planet. Sci. Lett.* **109**, 517 (1992).
19. A. Navrotsky and K. Bose, in *Processes of Deep Earth and Planetary Volatiles*, K. Farley, Ed. (American Institute of Physics, New York, 1995), pp. 221–228.
20. D. Toomey *et al.*, *Eos (Fall Suppl.)* **77**, 652 (1996).
21. D. Blackman *et al.*, *Geophys. J. Int.* **127**, 415 (1996).
22. J. S. Collier and M. C. Sinha, *J. Geophys. Res.* **97**, 14031 (1992).
23. L. M. Parson and I. C. Wright, *Tectonophysics* **263**, 1 (1996); B. Taylor, K. Zellmer, F. Martinez, A. Goodliffe, *Earth Planet. Sci. Lett.* **144**, 35 (1996).
24. J. A. Pearce *et al.*, in *Volcanism Associated with Extension at Consuming Plate Margins*, J. L. Smellie, Ed. (Geological Society, London, 1992), pp. 53–75; J. W. Hawkins, in *Active Margins and Marginal Basins of the Western Pacific*, B. Taylor and J. Natland, Eds. (American Geophysical Union, Washington, DC, 1995), pp. 125–173.
25. B. L. N. Kennett and E. R. Engdahl, *Geophys. J. Int.* **105**, 429 (1991).
26. W. Crawford, S. Webb, J. Hildebrand, *Eos (Fall Suppl.)* **77**, 478 (1996).
27. S. Billington, thesis, Cornell University, Ithaca, NY, (1980).
28. B. L. N. Kennett, *Seismic Wave Propagation in Stratified Media* (Cambridge Univ. Press, Cambridge, 1983); G. E. Randall, *Geophys. J. Int.* **118**, 245 (1994).
29. U. H. Faul, D. R. Toomey, H. S. Waff, *Geophys. Res. Lett.* **21**, 29 (1994).
30. We thank M. Bevis, W. Crawford, K. Draunidalo, S. Escher, T. Fatai, H. Gilbert, S. Helu, K. Koper, M. McDonald, J. McGuire, B. Park-Li, G. Prasad, E. Roth, A. Sauter, P. Shore, and L. Vuetibau for their assistance during the seismic experiment and at the data-processing stage and G. Abers and an anonymous referee for thoughtful reviews, which improved the manuscript. Broadband seismographs were obtained from the PASSCAL program of the Incorporated Research Institutions in Seismology (IRIS). Supported by the NSF under grants EAR-9219675,

COE-9314446, and EAR-9614502. This paper is Southern California Earthquake Center publication 386.

8 May 1997; accepted 18 August 1997

## Microscopic Molecular Diffusion Enhanced by Adsorbate Interactions

B. G. Briner,\* M. Doering, H.-P. Rust, A. M. Bradshaw

The diffusion of carbon monoxide molecules on the (110) surface of copper was investigated in the temperature range between 42 and 53 kelvin. The activation energy for thermal motion was determined directly by imaging individual molecular displacements with a scanning tunneling microscope. An attractive interaction between carbon monoxide molecules gave rise to the formation of dimers and longer chains. Carbon monoxide chains diffused substantially faster than isolated molecules although the chains moved by a sequence of single-molecule jumps. A higher preexponential factor in the Arrhenius law was found to be responsible for the observed efficiency of chain hopping.

Adsorbate diffusion is of fundamental importance for surface chemistry (1). It is often the rate-limiting step in catalysis because adsorbed atoms or molecules first have to reach a reaction partner or an active site (2) on the surface before a reaction can take place. Efforts to study diffusion on a microscopic scale are needed to understand how interactions with the surface and with neighboring adsorbates influence the way a particle diffuses. This information forms an indispensable basis to model diffusion on a macroscopic scale under the conditions that prevail in catalysis. This report focuses on the microscopic diffusion of CO molecules on Cu(110). Carbon monoxide is only weakly chemisorbed on Cu(110) (3), and helium scattering experiments have suggested very low diffusion barriers (4). Therefore, CO can serve as a test case to assess whether diffusion of the often weakly bound molecules that are of interest in surface chemistry is accessible to microscopic observation.

All experiments were performed with an Eigler-type, variable temperature scanning tunneling microscope (STM), which operates in an ultrahigh vacuum and can be cooled down to 4 K (5). We applied experimental techniques similar to those used in earlier STM-based studies on diffusion (6), but the present results differ in two ways from earlier findings. First, we observed that the activation energy for CO diffusion was substantially lower than the barrier heights that had been determined before with microscopic imaging techniques. This result in-

dicates that the STM can indeed be used to probe the motion of weakly bound species and that the artifacts of STM-induced adsorbate motion that were reported in (7) can be avoided. Second, our study went beyond the observation of single-particle diffusion. It was found that CO forms chains on Cu(110). These chains experienced considerable thermal mobility in the same temperature range in which the diffusion of isolated molecules was observed. By comparing the diffusion of single molecules with that of CO chains, we could investigate the influence of molecular interactions on the adsorbate mobility. Cluster diffusion was first investigated by field ion microscopy (FIM) (8). Although this technique is limited to the study of strongly bound transition metal adatoms, it could provide detailed information on the characteristics of cluster diffusion. In general, the rule that cluster mobility decreases strongly with increasing cluster size was confirmed, but FIM experiments have also demonstrated that there are exceptions to this rule. Iridium tetramers have been found to diffuse faster than trimers (9), and for rhenium on tungsten(211), dimers have been shown to be faster than single adatoms (10). The reason for this enhanced mobility is a reduction of the activation energy; adding an atom to a cluster can strengthen the cluster bonds at the expense of weakening the bonds to the substrate (11–13). We observed that CO chains also experienced an enhanced mobility, but in contrast to the metal clusters described above, no reduced activation energy for chain diffusion was found.

Samples were prepared by adsorbing CO onto the clean Cu(110) substrate at a temperature of about 60 K. We found that under these adsorption conditions, CO still has substantial mobility. This mobility is inferred

Fritz-Haber-Institut der Max-Planck-Gesellschaft, Faradayweg 4-6, 14195 Berlin, Germany.

\*To whom correspondence should be addressed. E-mail: briner@fhi-berlin.mpg.de

from the nonuniform adsorbate distribution shown in Fig. 1A, an image that was recorded after the CO-covered sample was cooled to 9 K. Isolated CO molecules appear as 0.4 Å deep depressions. CO is imaged on the close-packed rows of Cu(110), in accordance with photoelectron diffraction and STM studies that have indicated that CO adsorbs on top of the Cu atoms in the outermost substrate layer (14, 15). Besides isolated CO molecules, we find dimers and longer molecular chains in Fig. 1A. The chains are always oriented perpendicular to the close-packed rows and give evidence for an attractive interaction along the [001] direction of the substrate. Note that all chains appear in the STM image with local maxima between the individual adsorbates. These features could be observed repeatedly with different tips and tunneling parameters, and therefore, we suggest that they are related to a charge density perturbation resulting from substrate-mediated CO-CO bonding. This interpretation is in accordance with the observation that such a maximum disappears when thermally induced chain breaking occurs and reappears when the broken chain segments rejoin.

Carbon monoxide diffusion was studied in the temperature range between 42 and 53 K. To determine the molecular hopping rate, we first recorded a time-lapse series of STM images with a tunneling current of 100 pA and a bias of 50 to 100 mV (16). As an example, a 130 Å by 130 Å detail of a larger image that was obtained at 44 K is displayed in Fig. 1B. Molecules that have moved between individual images of a series were identified by calculating difference images. A color-coded image that represents the difference between Fig. 1B and a frame recorded 580 s later is shown

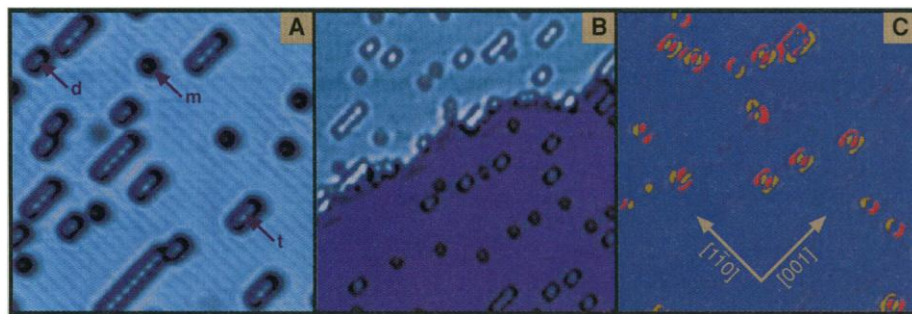


**Fig. 1.** (A) High-resolution image of CO adsorbed onto Cu(110) taken at 9 K (area = 100 Å by 100 Å, tip voltage  $V_{\text{tip}} = -20$  mV, and tunneling current  $I_T = 10$  nA). Carbon monoxide molecules (m), dimers (d), and trimers (t) are labeled. (B) Scanning tunneling microscope image of CO adsorbed onto Cu(110) recorded at 44 K ( $V_{\text{tip}} = -100$  mV and  $I_T = 100$  pA). The image displays one monatomic step. Adsorbate-related features closely correspond to those in (A). (C) Color-coded difference image between (B) and an image of the same area that was recorded after a delay of 580 s. Only molecules that have hopped are visible. Yellow and red indicate the initial and final adsorbate sites, respectively. The color coding highlights those parts of the adsorbate-related features that appear darker than the background in (B). Carbon monoxide chains that appear in the raw data as oval-shaped valleys surrounding a shallow ridge are visualized as double pairs of parallel red and yellow lines in (C). In contrast, isolated CO molecules that are reproduced as dark spots in the raw data appear in the difference image as a single pair of red and yellow arc segments.

in Fig. 1C. It reveals that various isolated CO molecules, dimers, and a chain of four molecules have changed their site. All displacements occurred exclusively in the [110] direction. The hopping rate  $\nu_s(T)$  (where  $s$  stands for single) at a constant temperature  $T$  was obtained by fitting the fraction of adsorbates  $n(t)/n_0$  that had not moved in the time interval  $t$  with the use of Poisson statistics:  $n(t)/n_0 = \exp(-\nu_s t)$ . Typically, the total number of molecules per data set amounted to  $n_0 = 500$ . The hopping rates that were determined at different temperatures were compiled in an Arrhenius plot (Fig. 2). We first concentrate on the data for isolated CO molecules; the results for dimers are discussed later. The temperature dependence of the diffusivity  $D = l^2 \nu_s / 2$  ( $l$  is the hopping distance) follows an Arrhenius law [ $D = D_0 \exp(-E_a/kT)$ ;  $D_0$  is the prefactor and  $k$  is the Boltzmann constant] (17), and thus, the data on Fig. 2 should fall on a line. The linear fit for single CO molecules corresponds to an activation energy of  $E_{\text{as}} = 97 \pm 4$  meV and a prefactor of  $D_{0s} = 2.5 \times 10^{-8 \pm 0.37}$  cm<sup>2</sup>/s.  $E_{\text{as}}$  is a reasonable fraction (15%) of the desorption energy (3).  $D_{0s}$  is quite low compared with the theoretical prediction that the prefactor should be about  $10^{-3}$  cm<sup>2</sup>/s (1). Some FIM studies have obtained prefactors that roughly agree with this prediction (8), but, in general, the experimental data for  $D_0$  have varied by more than six orders of magnitude (13). In addition, experiments on CO diffusion have reported similarly low values for  $D_0$  (18). If the conventional theoretical approach to describe  $D_0$  (1) is applicable for CO diffusion, the low prefactor that was found in these experiments corresponds to an attempt frequency of only  $3 \times 10^7$  cm<sup>2</sup>/s, a result that would indicate that only very few thermally accessible configura-

tions of the CO molecule can result in a hopping event.

A reliable test to ensure that the observed adsorbate motion is not induced by the STM is to vary the interaction time between the adsorbates and the probe tip (19). This test was done by first recording a reference series with short time intervals  $\Delta t$  between individual images. Subsequently, further images were obtained with identical scan parameters but separated by delays of up to  $12\Delta t$ . During the delay time, the tip was moved to the edge of the scan area and the scan was stopped. We found the number of adsorbate displacements on these latter images to be in full accordance with the reference data; that is, to within the statistical error, our measurements were not affected by tip-induced artifacts.

A comparison of the mobility of CO molecules, dimers, and trimers is shown in Fig. 3A. This graph illustrates that dimers and trimers diffuse with a substantially higher hopping rate than single molecules. The fit to the monomer data corresponds to a mean residence time of 2050 s. Carbon monoxide chains were observed to diffuse in sequential fashion by successive jumps of single molecules. Therefore, chain diffusion involves several time constants and is more difficult to model than monomer diffusion. To describe dimer and trimer diffusion, one needs to know

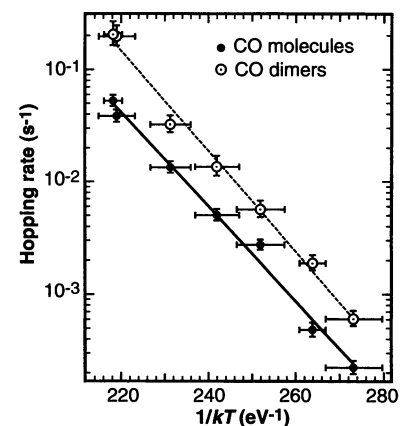


**Fig. 2.** Arrhenius plot of the hopping frequencies of CO molecules (filled circles) and CO dimers (open circles with dots) in the temperature range between 42 and 53 K. The parameters  $E_a$  and  $D_0$  for the two linear fits are given in the text together with statistical error limits that were derived from the fitting procedure. The horizontal error bars indicate the estimated temperature uncertainty, which includes a possible gradient between the sample position and the sensor location and a temperature drift of 0.2 to 0.5 K during data acquisition. Because of this uncertainty, the effective error of  $D_0$  increases to  $10^{\pm 1.5}$ . It is important to note that the rates of dimer and monomer hopping were obtained from the same data sets. Therefore, the error of the ratio  $D_{0d}/D_{0s}$  is not affected by the relatively large temperature uncertainty.

the difference in free energy between the “straight” and the “open” configurations (Fig. 3B) (chains in bent configurations are termed “open” because creating a bent chain is equivalent to partially breaking a CO–CO bond). From the observation of 3576 straight and 139 open dimers at  $T = 44$  K, we determined a free energy difference of  $\Delta F_d = 14.9 \pm 0.4$  meV between the two dimer states. A similar calculation for trimers resulted in a slightly lower energy difference of  $13.8 \pm 0.6$  meV. Knowing these values, we can derive the hopping times of the elementary steps of chain motion (sketched on Fig. 3B) from a fit to the experimental data (Fig. 3A) (20). We found that dimer breaking takes an average time of  $\nu_{db}^{-1} = 511$  s. The rejoining step was much faster ( $\nu_{dj}^{-1} = 20$  s). A similar fit for trimers resulted in  $\nu_{tb}^{-1} = 525$  s and  $\nu_{tj}^{-1} = 27$  s. Trimer motion also included a site exchange of the molecule in the middle of the chain. This swapping process, which interchanges equivalent open trimer configurations, was found to be very fast. We could only determine an upper limit of  $\nu_{ts}^{-1} = 14$  s to the swapping time at 44 K, indicating that this step is at least twice as fast as trimer joining. Because swapping

between open chain configurations is so efficient, even relatively long chains can diffuse faster than single molecules. For example, the hopping of a chain of seven CO molecules at 44 K took only 134 s (Fig. 4), which is 15 times less than the average hopping time for single molecules.

To answer the question, why can small chains diffuse faster than single CO molecules, one has to determine the effective chain hopping rate  $\bar{\nu}$  ( $\bar{\nu}^{-1}$  is the time it takes a chain in the straight configuration to shift by one lattice constant), because in the limit of long time intervals,  $\bar{\nu}$  determines the efficiency of mass transport. According to (21),  $\bar{\nu}$  can be derived from the hopping rates of the elementary jump processes. For the data set shown in Fig. 3A, we found  $\bar{\nu}_d^{-1} = 531$  s for dimers and  $\bar{\nu}_t^{-1} \leq 729$  s for trimers. For comparison with monomer hopping, we included the effective hopping rates of dimers that were obtained at different temperatures in the Arrhenius plot (Fig. 2, open circles). The linear fit to the dimer data resulted in an activation energy of  $E_{ad} = 103 \pm 5$  meV and a prefactor of  $D_{0d} = 3.6 \times 10^{-7 \pm 0.4}$  cm<sup>2</sup>/s. Obviously, what accounts for the difference between monomer and dimer diffu-

sion is a substantially increased prefactor:  $D_{0d}/D_{0s} = 1.44 \times 10^{1 \pm 0.55}$ . There are two possible reasons for the observed increase in  $D_0$ . First, the attempt frequency for dimer breaking could be higher if the presence of neighboring adsorbates increases the energy of the frustrated translation. We consider this to be unlikely, however, because of the large change in frequency required. Second,  $D_0$  increases if the entropy of a molecule that is bound in a dimer is lowered compared with an isolated molecule. To test for the presence of such entropy effects, we also determined the free energy difference between open and straight dimers at  $T = 48.6$  K. We found a slightly lower value of  $\Delta F_d = 14.2 \pm 0.6$  meV compared with the result at  $T = 44$  K; that is, the entropy of the open dimer configuration (which approximates the situation of two independent molecules) is indeed higher than the entropy of a straight dimer ( $\Delta S = 0.15$  meV/K). Similar entropy effects have been found to be responsible for the temperature-dependent adsorption site conversion of CO on Ni(100) (22). The interpretation that a reduced entropy accounts for the enhanced chain mobility is in line with our observation that all small CO chains experience a higher hopping rate than single molecules (23). This phenomenon contrasts with the diffusion of metal clusters, which is controlled by the strong interactions between adatoms.

In conclusion, these experiments on CO diffusion show that weak adsorbate interactions can lead to unpredicted diffusion phenomena. Provided that the findings of the present study remain valid under the conditions that typically prevail in catalysis (high temperature and high adsorbate coverage), diffusion stimulated by adsorbate interactions could potentially enhance the efficiency of surface chemical reactions by increasing the rate of mass transport.

## REFERENCES AND NOTES

1. R. Gomer, *Rep. Prog. Phys.* **53**, 917 (1990).
2. T. Zambelli, J. Wintterlin, J. Trost, G. Ertl, *Science* **273**, 1688 (1996).
3. K. Horn, M. Hussain, J. Pritchard, *Surf. Sci.* **63**, 244 (1977); J. Ahner, D. Mocuta, R. D. Ramsier, J. T. Yates Jr., *J. Chem. Phys.* **105**, 6553 (1996).
4. M. F. Bertino, F. Hofmann, W. Steinhögl, J. P. Toennies, *J. Chem. Phys.* **105**, 11297 (1996).
5. H.-P. Rust, J. Buisset, E. K. Schweizer, L. Cramer, *Rev. Sci. Instrum.* **68**, 129 (1997).
6. E. Ganz, S. K. Theiss, I.-S. Hwang, J. A. Golovchenko, *Phys. Rev. Lett.* **68**, 1567 (1992); I.-S. Hwang, S. K. Theiss, J. A. Golovchenko, *Science* **265**, 490 (1994); B. S. Swartzentruber, *Phys. Rev. Lett.* **76**, 495 (1996); T. Zambelli, J. Trost, J. Wintterlin, G. Ertl, *ibid.*, p. 795; J. M. Gomez-Rodriguez, J. J. Saenz, A. M. Baro, J.-Y. Veullien, R. C. Cinti, *ibid.*, p. 799; J. Wintterlin, R. Schuster, G. Ertl, *ibid.* **77**, 123 (1996); J. V. Barth, T. Zambelli, J. Wintterlin, R. Schuster, G. Ertl, *Phys. Rev. B* **55**, 12902 (1997).
7. P. Ebert, M. G. Lagally, K. Urban, *Phys. Rev. Lett.* **70**, 1437 (1993); Y. W. Mo, *ibid.* **71**, 2923 (1993); M. Bott, M. Hohage, M. Morgenstern, T. Michely, G. Comsa, *ibid.* **76**, 1304 (1996); J. Li, R. Berndt, W. D. Schneider, *ibid.*, p. 1888.

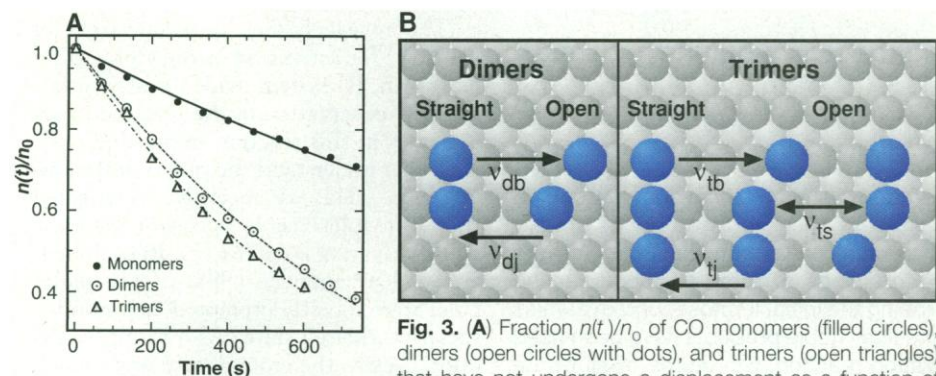


**Fig. 3.** (A) Fraction  $n(t)/n_0$  of CO monomers (filled circles), dimers (open circles with dots), and trimers (open triangles) that have not undergone a displacement as a function of time. Data were taken at a sample temperature of 44 K. Fit curves are discussed in the text. This figure illustrates that it takes significantly longer for single molecules to leave their site than it does for small chains to do so. (B) Sketch of the observed dimer and trimer configurations. Transitions between the different configurations are labeled.

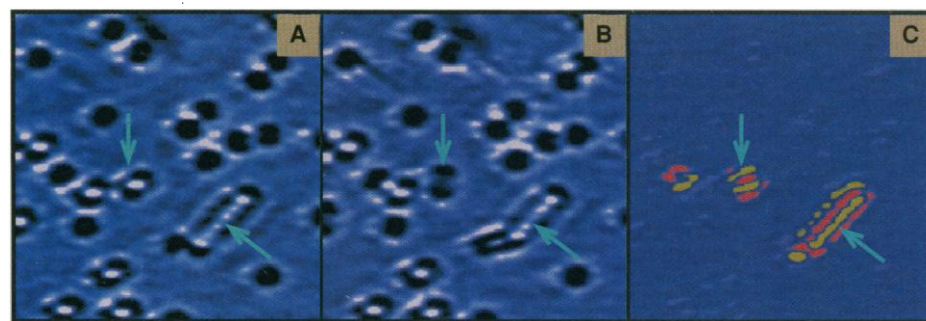


**Fig. 4.** Illustration of chain hopping at 44 K [topography images (A and B) and difference image (C)]. The difference image shown in the right panel was recorded after a delay time of 134 s. It is color-coded in the same way as Fig. 1C. The top arrow indicates a CO dimer and the bottom arrow indicates a chain of seven CO molecules. The dimer is shown to move in a sequential fashion by successive breaking and rejoining steps.

8. T. T. Tsong, *Rep. Prog. Phys.* **51**, 759 (1988); G. Ehrlich, *Surf. Sci.* **246**, 1 (1991); G. L. Kellogg, *Appl. Surf. Sci.* **87/88**, 353 (1995).
9. S. C. Wang and G. Ehrlich, *Surf. Sci.* **239**, 301 (1990).
10. K. Stolt, W. R. Graham, G. Ehrlich, *J. Chem. Phys.* **65**, 3206 (1976).
11. P. J. Feibelman, *Phys. Rev. Lett.* **58**, 2766 (1987).
12. D. W. Bassett, *J. Phys. C* **9**, 2491 (1976).
13. G. L. Kellogg, T. T. Tsong, P. Cowan, *Surf. Sci.* **70**, 485 (1978).
14. P. Hofmann *et al.*, *ibid.* **337**, 169 (1995).
15. M. Doering, J. Buisset, H.-P. Rust, B. G. Briner, A. M. Bradshaw, *Faraday Discuss. Chem. Soc.* **105**, 163 (1996).
16. Several movie sequences of STM images have been posted on our Web site (<http://www.fhi-berlin.mpg.de/of/of.html>) to provide a more detailed impression of the characteristics of CO diffusion.
17. Strictly speaking, this expression is only correct in a limited temperature range, because  $D_0$  is also weakly temperature dependent. Details can be found in (7).
18. B. Poelsma, L. K. Verheij, G. Comsa, *Phys. Rev. Lett.* **49**, 1731 (1982); J. E. Reutt-Robey, D. J. Doren, Y. L. Chabal, S. B. Christman, *J. Chem. Phys.* **93**, 9113 (1990); L. R. Becerra, C. A. Klug, C. P. Slichter, J. H. Sinfelt, *J. Phys. Chem.* **97**, 12014 (1993).
19. A further test for such STM-induced artifacts is to decrease the barrier resistance until individual CO molecules can be manipulated with the probe tip. We found that this happened typically at  $R < 2$  Mohm. A repulsive tip-adsorbate interaction was observed, in accordance with other reports on molecular manipulation (24, 25). Because all images of a time-lapse series are scanned in the same direction, repulsive interactions deplete the sampled area by shuffling the adsorbates to the edges of the scan window. Such an effect was never observed for the tunneling conditions ( $R = 0.5$  to 1 Gohm) used in the diffusion experiments.
20. The fits take into account the fact that "looplike" hopping sequences that bring the adsorbates back to their original sites can be overlooked in the experiment because of the finite time delay between sequential images. This effect, which increases the fraction of adsorbates that apparently have not moved, is much more important for chain hopping than for monomer hopping.
21. D. A. Reed and G. Ehrlich, *J. Chem. Phys.* **64**, 4616 (1976).
22. B. N. J. Persson, *Chem. Phys. Lett.* **149**, 278 (1988); A. Grossmann, W. Erley, H. Ibach, *Phys. Rev. Lett.* **71**, 2078 (1993).
23. Longer CO chains were also found to be very mobile, but it is difficult to quantitatively determine their hopping rate because they tend to break up easily.
24. T. A. Jung, R. R. Schlittler, J. K. Gimzewski, H. Tang, C. Joachim, *Science* **271**, 181 (1996).
25. B. G. Briner, M. Doering, H.-P. Rust, A. M. Bradshaw, *Phys. Rev. Lett.* **78**, 1516 (1997).
26. We acknowledge helpful discussions with H. Conrad and R. Liebenow.

29 May 1997; accepted 8 August 1997

temperature matrices (2, 6) to slow down the reaction.

In the gas phase, photolysis of  $\text{CpRh}(\text{CO})_2$  ( $\text{Cp} = \text{C}_5\text{H}_5$ ) yields the highly reactive  $\text{CpRhCO}$ , which reacts with alkanes at rates close to the gas-kinetic values (Fig. 1A) (4). Low-temperature matrix work also showed the formation of CO-loss products (2, 6). In liquid krypton solution, the solvated complex  $\text{Cp}^*\text{Rh}(\text{CO})\text{-Kr}$  ( $\text{Cp}^* = \text{C}_5\text{Me}_5$ , Me = methyl) is the first species observed. The alkane must then displace Kr before the final activation step can take place (5). These experiments established that the first step involves loss of a CO ligand to generate a coordinatively unsaturated intermediate. It is difficult, however, to generalize the results to room-temperature neat alkane solution because of the extreme changes in reaction conditions. In contrast to earlier work, our goal has been to study the reaction under the most relevant conditions, room-temperature alkane solution. To accomplish this, and to overcome the reaction-rate measurement limitations inherent in microsecond spectroscopy, we used ultrafast spectroscopy with picosecond (7) and femtosecond (8) time resolution, which allows access to the inter- and intramolecular processes that take place on time scales faster than diffusion.

The relatively low quantum yield of  $\sim 1\%$  (9) for activation in the  $\text{CpM}(\text{CO})_2$  ( $\text{M} = \text{Rh}, \text{Ir}$ ) system made ultrafast infrared (IR) observation of the reactive intermediates in this reaction impossible (10). To better understand the origin of the low quantum yield, we recently investigated the ultraviolet-visible spectroscopy of a C-H activating complex (7). In cyclohexane and *n*-pentane,  $\sim 99\%$  of the molecules were directly promoted to a nondissociative excited state. As a result, relaxation back to the ground state was a much more favorable process than CO loss.

Identification and subsequent understanding of the reaction intermediates are required to build a detailed picture of the overall bond-activation reaction. In our initial study of the photochemistry of C-H activation, we used ultrafast IR spectroscopy to monitor the reaction with  $\text{Tp}^*\text{Rh}(\text{CO})_2$  ( $\text{Tp}^* = \text{HB-Pz}_3^*$ ,  $\text{Pz}_3^* = 3,5$ -dimethylpyrazolyl) (Fig. 1B), taking advantage of its relatively high quantum yield ( $\sim 30\%$ ) for the formation of activated product (11). In cyclohexane,  $\text{Tp}^*\text{Rh}(\text{CO})_2$  shows peaks at 1981 and 2054  $\text{cm}^{-1}$  due to the antisymmetric and symmetric stretching modes of the two CO ligands. Upon irradiation, the static Fourier transform IR (FTIR) spectrum exhibits only a decrease in the intensity of the parent peaks and the corresponding formation of the final C-H activated product at 2032  $\text{cm}^{-1}$  [see figure 1 of (8)]. On the

## The Mechanism of a C-H Bond Activation Reaction in Room-Temperature Alkane Solution

Steven E. Bromberg, Haw Yang, Matthew C. Asplund, T. Lian,\*  
B. K. McNamara,† K. T. Kotz, J. S. Yeston, M. Wilkens,  
H. Frei,‡ Robert G. Bergman,‡ C. B. Harris‡

Chemical reactions that break alkane carbon-hydrogen (C-H) bonds are normally carried out under conditions of high temperature and pressure because these bonds are extremely strong ( $\sim 100$  kilocalories per mole), but certain metal complexes can activate C-H bonds in alkane solution under the mild conditions of room temperature and pressure. Time-resolved infrared experiments probing the initial femtosecond dynamics through the nano- and microsecond kinetics to the final stable products have been used to generate a detailed picture of the C-H activation reaction. Structures of all of the intermediates involved in the reaction of  $\text{Tp}^*\text{Rh}(\text{CO})_2$  ( $\text{Tp}^* = \text{HB-Pz}_3^*$ ,  $\text{Pz}_3^* = 3,5$ -dimethylpyrazolyl) in alkane solution have been identified and assigned, and energy barriers for each reaction step from solvation to formation of the final alkyl hydride product have been estimated from transient lifetimes.

Since the initial discovery that the strong C-H bonds in alkanes undergo oxidative addition to certain transition metal com-

plexes, the quest to understand and utilize this "C-H activation" reaction (Fig. 1, A and B) has been the focus of intense research effort (1). Insights into the individual steps involved in metal-mediated C-H activation reactions have been obtained from spectroscopic techniques with microsecond time resolution, with the goal of identifying the reaction intermediates (2, 3). However, the extremely rapid reaction rate prevents these established methods from monitoring the earliest kinetics at room temperature and requires that the experiments be performed in the gas phase (4), in liquefied noble gases (5), or in low-

S. E. Bromberg, H. Yang, M. C. Asplund, T. Lian, B. K. McNamara, K. T. Kotz, J. S. Yeston, M. Wilkens, R. G. Bergman, C. B. Harris, Department of Chemistry, University of California at Berkeley, and Chemical Sciences Division, Lawrence Berkeley National Laboratory, Berkeley, CA 94720, USA.

H. Frei, Laboratory of Chemical Biodynamics, M. S. Calvin Laboratory, Lawrence Berkeley National Laboratory, Berkeley, CA 94720, USA.

\*Present address: Department of Chemistry, Emory University, Atlanta, GA 30322, USA.

†Present address: Pacific Northwest National Laboratory, Post Office Box 999, Richland, WA 99352, USA.

‡To whom correspondence should be addressed.